Apoptosis (2008) 13:1267–1280
DOI 10.1007/s10495-008-0255-0

ORIGINAL PAPER

Oxidative stress by *Helicobacter pylori* causes apoptosis through mitochondrial pathway in gastric epithelial cells

Miryam Calvino-Fernández · Selma Benito-Martínez · Trinidad Parra-Cid

Published online: 3 September 2008

Abstract *Helicobacter pylori* is a gram negative bacterium that infects the human stomach of approximately half of the world's population. It produces oxidative stress, and mitochondria are one of the possible targets and the major intracellular source of free radicals. The present study was aimed at determining mitochondrial alterations in *H. pylori*-infected gastric epithelial cells and its relationship with oxidative stress, one of the recognized causes of apoptotic processes. Cells were treated with a strain of *H. pylori* for 24 h. Cellular oxidative burst, antioxidant defense analysis, mitochondrial alterations and apoptosis-related processes were measured. Our data provide evidence on how superoxide acts on mitochondria to initiate apoptotic pathways, with these changes occurring in the presence of mitochondrial depolarization and other morphological and functional changes. Treatment of infected cells with Vitamin E prevented increases in intracellular ROS and mitochondrial damage consistent with *H. pylori* inducing a mitochondrial ROS mediated programmed cell death pathway.

Keywords Apoptosis · Gastric epithelial cells · *Helicobacter pylori* · Mitochondria · Reactive oxygen species

Introduction

Helicobacter pylori (*H. pylori*) is a highly successful human pathogen that infects approximately half of the world's population [1, 2]. *H. pylori* infection has been implicated in the pathogenesis of chronic gastritis, peptic ulcer and more rarely, gastric carcinoma and mucosa-associated lymphoid tissue lymphoma (MALT) [1–3], but the mechanisms leading to these disease manifestations remain unclear. The bacterium induces a state of chronic gastric mucosa inflammation due to the local immune response inefficiency in eliminating this microorganism with the subsequent persistent infection. The evolution of this inflammatory state is related to both toxicity of bacterial strain and to host's defenses. Strains bearing the cag pathogenicity island, which includes the cagA gene, have shown to be associated with increased gastric inflammation [4], and both peptic ulcer disease and gastric cancer [5]. Furthermore, there are clinical findings that strongly suggest that factors such as stress, diet, smoking, sanitization, or host genetic background contribute to the pathogenesis of the infection [6].

Several reports have described an association between *H. pylori* infection and apoptosis in gastric epithelial cells both "in vitro" [7, 8] and "in vivo" experiments [9–11].

Apoptosis, or programmed cell death, is essential in the development and homeostasis of multicellular organisms. This mechanism plays a major role in cellular growth regulation, immune response development, and redundant or abnormal cells clearance [12], but apoptosis may also work as a defense system against bacterial and viral infections [13]. *H. pylori* infection is believed to increase epithelial proliferation and to be linked to apoptosis to maintain cellular homeostasis.

Apoptosis is a passive way of cell suicide that can be triggered by a variety of internal and external signals [14]. Programmed cell death generally represents a response to gross injury induced either by an overdose of cytotoxic agents (free radicals, drugs…), by serious injury (traumatisms,

M. Calvino-Fernández (✉) · S. Benito-Martínez · T. Parra-Cid
Hospital Universitario de Guadalajara, Unidad de Investigación, C/Donante de Sangre s/n19002, Guadalajara, Spain
e-mail: mcalvino@sescam.jccm.es

radiations…) [15] or by intracellular pathogens (*Mycobacterium tuberculosis*, *Mycobacterium bovis*…) [16]. Some authors have demonstrated that programmed cell death in cultured gastric epithelial cells is due to the bacteria direct effect and to the proinflammatory cytokines that are released during infection [6, 17].

Apoptosis is associated with profound structural changes and biochemical events leading to irreversible cell destruction. Morphological alterations include cell shrinkage because of disordered volume regulation [18], loss of membrane integrity [19], chromatin condensation and emission of apoptotic bodies [20]. Functional alterations and biochemical events include loss of lipid asymmetry manifested by the translocation of phosphatidylserine residues to the outer layer of the plasma membrane [21], lipidic peroxidation, activation of caspases [22] and DNA fragmentation into oligonucleosomal fragments [23].

Preliminary studies have described that the apoptosis in *H. pylori* infection is induced by a pathway involving Fas/Fas ligand system [8, 24, 25]; although, it was recently reported [26, 27] that a mitochondrial pathway contributed to this process. Mitochondria are considered as pivotal organelles in the process of most cell-death pathways [28–30], liberating proapoptotic substances such as cytochrome *c* (cyt *c*).

The present study was aimed at characterizing ROS changes and mitochondrial alterations during infection with *H. pylori* in gastric epithelial cells.

Materials and methods

Cell line and culture condition

Human gastric carcinoma-derivated AGS epithelial cells (ATCC® CRL 1739; Manassas, Virginia, USA) were grown in RPMI medium 1640 (Sigma-Aldrich Inc, St. Louis, MO, USA) supplemented with 10% fetal bovine serum (FBS) (Biochrom AG, Berlin, Germany), 2 mM L-glutamine, sodium bicarbonate 2 g/l and antibiotics (ampicillin 125 μg/ml, gentamycin 40 μg/ml and cloxacillin 125 μg/ml) at 37°C and 5% CO_2.

Bacteria strain

Lyophilized *H. pylori* stock (ATCC® 700824, Manassas, Virginia, USA) [cagA+/vacA s1/m1] was reconstituted with 4 ml Trypticase Soy Broth (BD, San Jose, CA) and cultured on sheep blood agar (Biomedics, Madrid, Spain) at 37°C under microaerophilic atmosphere generated with Campygen™ packets (OXOID Ltd, Hampshire, England). Cultures were maintained for three days prior to passing; bacteria were used between passages 2 and 15 from frozen stocks. Cultures were routinely screened for urease activity.

Culture of AGS cells with *H. pylori*

When AGS epithelial cells were confluent, they were washed twice and then fresh medium with 0.5% FBS and free of antibiotics was added. The appropriate numbers of bacteria were calculated by comparison of turbidity to McFarland standards [31], being 1:200 the used MOI (Multiplicity Of Infection) in all the assays (bacterial density, 1×10^8 CFU/ml) (CFU: Colony Forming Units). Cocultures were then placed at 37°C and 5% CO_2.

AGS cells were supplemented with alpha-tocopheril acetate (Vit E) (Ephynal®, Roche, Basel, Switzerland) (10^{-4} M) 30 minutes before adding the bacterium. AGS and bacteria were cocultured for 24 h, with and without Vit E.

For flow cytometry (FC) assays, AGS cells were cultured in the presence of RPMI only (used as control) or with suspensions of *H. pylori*. Supernatants were collected in order to recover the cells that were detached during treatment. After washing with physiological serum, adherent cells were harvested with 2.2 mM EDTA in trypsin (Sigma-Aldrich Inc, St. Louis, MO, USA) (this treatment does not affect our results), mixed with supernatant and labelled as it will be described.

FC experiments were performed in a Becton Dickinson FACScan (BD Biosciences, San Diego, CA, USA) with 488 nm-line laser and FL1 (530/30 nm band pass filter), FL2 (585/42 nm band pass filter) and FL3 (670 nm long pass filter) detectors. At least 10,000 cells were examined in each assay using Cell Quest program. Results were expressed in Mean Fluorescence Intensity (MFI).

Confocal Microscopy (CM) assays were done by direct labelling of the adherent cells in plates. All images were taken using a ×20 objective and amplified with different zooms. Data for each experiment were obtained after counting the cells in at least three fields. Images are then analysed via the Olympus FV 1000 software (Olympus Fluoview, version 1.6, Tokyo, Japan): after subtracting background, total fluorescence of each field was divided by the total number of cells, and the results were then presented as MFI/cell.

Cellular oxidative burst and antioxidant defense analysis

2′,7′-dichlorofluorescein diacetate (DCFH-DA) oxidation

DCFH-DA is a nonpolar substance and freely diffuses through the cell membrane; within the cell it is hydrolysed

to fluorescein (DCFH), a polar compound that is trapped within the cell. DCFH is a substrate that is easily oxidized to DCF by hydrogen peroxide (and other substances generated by oxidative metabolic burst) emitting fluorescence at 560 nm [32]. This fluorescence intensity is directly proportional to these oxidant components. Cells both infected and non-infected with the bacteria were incubated for 45 min at 37°C with 5 μM DCFH-DA (Molecular Probes, Oregon, USA). Cells were detached by trypsinization, washed and cellular fluorescence intensity was measured by FC. Results at 10^8UFC/ml with and without Vit E were corroborated by CM images.

Monobromobimanes (mBBr)

mBBr are non fluorescent molecules until they are conjugated with several low molecular weight thiols, mainly glutathione. Reduced glutathione (GSH) protects cells against oxidative injury produced in different metabolic processes [33]. GSH depletion in *H. pylori* treated cells, was assayed with mBBr. Briefly, cocultures were incubated with 2 μM mBBr (Molecular Probes, Oregon, USA) at 37°C and 5% CO_2 for 10 min. After washing twice, staining was observed by CM.

NAD(P)H

NAD(P)H quantity is in relationship with the complex I redox status of the mitochondrial electronic transport chain and its oxidation reflects the electrons release towards oxygen molecules causing an interruption in the normal flow of respiratory chain and superoxide anion ($O_2^{\bullet -}$) synthesis. Cells emit blue fluorescence in a proportional way to their content in NAD(P)H molecules when they are excited with an UV laser (360 nm) [34]. In our experiments, cells were trypsinized and resuspended in 0.5% RPMI and then acquired in a sorter (FACStar Plus, Becton Dickinson). Seventy percent ethanol was used as a control; the fluorescence of a control sample is set as 100% and a zero NAD(P)H value is generated by analysing a sample of cells fixed in 70% ethanol, which is devoid of NAD(P)H [35]. Their fluorescence was analysed using a 450 centered band-pass filter after excitation with UV laser.

Oxidative burst and morphological and functional alterations of mitochondria

Mitochondrial superoxide determination

MitoSOX Red is a cell-permeable dye that is oxidized in the presence of mitochondrial superoxide anion $O_2^{\bullet -}$, the main free radical produced in mitochondria. After oxidation it becomes fluorescent emitting a red fluorescence after 488 nm laser excitation. Cells were incubated for 10 min with MitoSOX Red reagent 5 μM (Molecular Probes, Oregon, USA) in 0.5 ml of Hank's Balanced Salt Solution (Sigma-Aldrich Inc, St. Louis, MO, USA) with calcium and magnesium ($CaCl_2$ 140 mg/l, $MgCl_2$-6 · H_2O 100 mg/l and $MgSO_4$-7 · H_2O 100 mg/l), and washing twice cultures were observed in a CM using a 580 centered band-pass filter.

Mitochondrial membrane potential (Δψm) assay

MitoProbe JC-1 Assay (Molecular Probes, Oregon, USA) was used. JC-1 (5,5′,6,6′-tetrachloro-1,1′,3,3′-tetraethylbenzimidazoly-carbocianine iodide) is a cationic dye that exhibits potential-dependent accumulation in mitochondria [36], indicated by a fluorescence emission shift from green (∼525 nm) to red (∼590 nm). In normal cells, due to the electrochemical potential gradient, the JC-1 dye concentrates in the mitochondrial matrix, where it forms red fluorescent aggregates. Any event that dissipates the mitochondrial membrane potential (e.g. apoptosis) prevents the accumulation of the JC-1 dye in the mitochondria. The dye is dispersed throughout the entire cell, resulting in a shift from red fluorescence (J-aggregates) to green fluorescence (JC-1 monomers). AGS epithelial cells with differently treated groups were stained with 2 μM JC-1 in 1 ml of RPMI 0.5% FBS for 15 min at 37°C and 5% CO_2, washed twice and analysed by CM. Red and green fluorescences were collected through appropriated filters and the red/green ratio was calculated as an index of Δψm.

Examination of lipidic oxidation and mitochondrial network structure

Nonyl acridine orange (NAO) presents high affinity by cardiolipin [29], a polyunsaturated acidic glycerophospholipid exclusively found in the inner mitochondrial membrane (IMM). When NAO is bound to cardiolipin after 488 nm laser excitation, it emits fluorescence at 630 nm whose quantity is related to mitochondrial cardiolipin content providing a peroxidation index. Therefore, a decreased red fluorescence is, among other reasons, related to decreased mitochondrial cardiolipin content as a consequence of peroxidation processes [37]. Cultures were directly labelled in wells with 100 nM NAO (Molecular Probes, Oregon, USA) for 10 min at 37°C in 0.5 ml of 0.5% FBS RPMI solution. After washing twice, CM images were taken and fluorescence intensity by cell was calculated.

This NAO bound to phospholipids of mitochondria membranes allows CM observation of mitochondrial network structures and the changes caused by bacterium incubation.

Apoptosis assays

A. Caspase-2 FLICA Assay (Sigma-Aldrich Inc, St. Louis, MO, USA) contains green carboxy-fluorescein (FAM), a derivate of benzyloxycarbonyl valylaspartyl-valylalanylaspartic acid (VDVAD) fluoromethyl ketone (FMK), a potent inhibitor with a preference for caspase-2 activity. Because the FAM-VDVAD-FMK in the cell becomes covalently bound to the enzyme, it remains in the cell, while unbound reagent is washed away. The green fluorescence signal is a measure of active caspase-2 that was present in the cell at the time the reagent was added [38]. Assays were performed both by FC and by CM, according to the manufacturer instructions. Briefly, for CM images cells were directly labelled in 6-well plates with FLICA reagent 10× for 2 h at 37°C and 5% CO_2. These labelled cells were harvested by trypsinization and analysed by FC.
B. Staining cells with acridine orange (AO) enables the determination of apoptosis based on nuclear morphology [29]. AO is a cell-permeable dye that enters all cells and intercalates DNA to appear green with a green homogenous fluorescence; the nuclear condensation (feature of apoptotic cells) causes an intensification of this fluorescence and loss of homogeneous pattern [16]. Apoptotis cells were enumerated by counting 500 cells at multiple randomly selected fields. AGS epithelial cells were stained with 1 μM AO (Sigma-Aldrich Inc, St. Louis, MO, USA) for 10 min at 37°C and 5% CO_2, washed twice and analysed by CM.
C. DNA Fragmentation Assay. *Suicide-Track*™ *DNA Ladder Isolation kit* (Calbiochem, USA) was used. The principle involves detecting the cytoplasmic histone-associated DNA fragments (mononucleosome and oligonucleosomes) formed during apoptosis. Briefly, cells were trypsinized and centrifugated (both adherent cells and supernatants). The pellet was resuspended in 500 μl of Extraction Buffer, incubated for 30 min on ice and centrifugated at 15.000 g/5 min at room temperature. Carefully, supernatant was removed and transferred to a clean tube, discarding in this way the high molecular weight chromatin. It was added 20 μl of Solution #2 and was incubated for 60 min. Afterwards 25 μl of Solution #3 was added, gently mixed and incubated at 50°C for 3 h. The DNA was precipitated with the kit reagents provided and dissolved in 50 μl of Resuspension Buffer. Samples and DNA marker were resolved in 1.5% agarose gel at 50 V for 2 h containing 10.000X SYBR Green®I in 1 × Tris-Acetate-EDTA buffer. The bands were visualized using an UV-illumination (GELPRINTER PLUS, Madrid, Spain).

Statistical analysis

Experiments were carried out at least in triplicate and data in text and figures are expressed as mean values ± standard deviation (SD). Statistical analysis was performed using the statistical software, SPSS version 12.0 (SPSS Inc., Chicago, IL, USA). Differences between groups were analysed with a *t*-test (T-student) or a non-parametric test (Wilcoxon test). A *p*-value of less than 0.05 (2-tailed test) was considered statistically significant.

Results

Reactive oxygen species (ROS) production

Firstly, we verified that AGS cell line was sensitive to *H. pylori* through an alteration in its oxidative status. Therefore, AGS were incubated with various bacterial densities (1×10^4 CFU/ml, 1×10^5 CFU/ml, 1×10^6 CFU/ml, 1×10^7 CFU/ml, 1×10^8 CFU/ml and 2×10^8 CFU/ml) for 12, 24 and 48 h and we analysed free radicals synthesis. The oxidation of DCFH-DA, a non-fluorescence probe, to DCF, a fluorescence probe was then measured.

The data obtained by FC showed a fluorescence increase directly proportional to the bacterial density and time of incubation ($P \leq 0.05$); except for the highest density (2×10^8 CFU/ml) and for the longer infection time (48 h) where the culture cells were detached in considerable proportions (they were death by necrosis, measured with Trypan Blue) and the emission of fluorescence was lost.

At 24 h we found the most relevant alterations. Our experiments showed that *H. pylori* increased DCF fluorescence in a dose dependent manner, from 1.5-fold increase with 1×10^4 CFU/ml to 2.5-fold increase with 10^8 CFU/ml, compared to controls (all $P \leq 0.05$) (Fig. 1, top panel). We decided to work with 10^8 CFU/ml since it is related to one of the most used MOI in the bibliography (1:200) [31, 39] and because the free radicals synthesis almost completely disappeared after Vit E addition. Data were obtained by FC and corroborated by CM images (Fig. 1, low panel).

ROS include radical species such as peroxide anion, hydroperoxyl radical, hydroxyl, carbonate, peroxyl and alkoxyl radical, and non-radical species such as H_2O_2, HOCl, fatty acid hydroperoxides, and singlet oxygen. These oxidant species can be generated in either extramitochondrial or mitochondrial locations. Mitochondria, however, are one of the most important sources of intracellular ROS, namely superoxide.

We used MitoSOX Red, a non-fluorescent reduced probe, to evaluate specifically intramitochondrial sources of free radicals since this substrate is exclusively oxidized

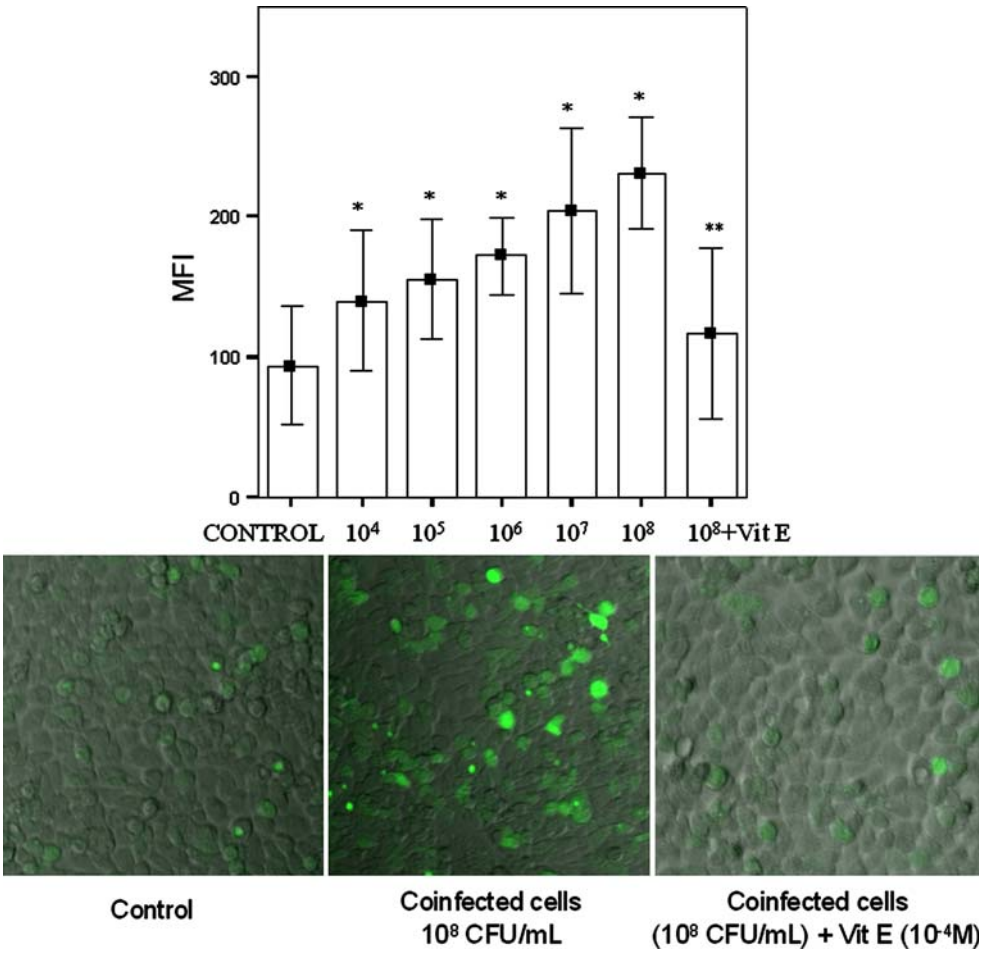

Fig. 1 Cell oxidative burst evaluated by FC or CM and DCFH-DA labelling. A dose-response graphic (where each value corresponds to the mean ± SD of four separate experiments) shows a DCF fluorescence increase in *H. pylori*-treated cells for 24 h (140.0 ± 31.7 MFI; 155.5 ± 26.9 MFI; 172.0 ± 17.2 MFI; 204.3 ± 37.0 MFI; 231.3 ± 24.4 MFI versus 93.7 ± 26.2 MFI) (*$P \leq 0.05$). Antioxidant addition at 1×10^8 CFU/ml bacterial density, decreased fluorescence values (116.8 ± 38.3 MFI) (**$P \leq 0.05$ compared to the coculture), as it is also displayed in the images recorded by confocal microscopy (Olympus). Original magnification, ×20

by $O_2^{\bullet -}$. Oxidized MitoSOX Red's fluorescence is therefore proportional to the amount of mitochondrial $O_2^{\bullet -}$. In our experiments, CM images (Fig. 2) of MitoSOX Red reagent showed higher fluorescent values in *H. pylori* cocultures (7.79 ± 0.89 MFI versus 4.35 ± 0.49 MFI) ($P \leq 0.05$), indicating that, at least, a proportion of free radicals synthesis that the bacterium causes, are taking place in mitochondria. Since our hypothesis is based on the assumption that the oxidative stress is the cause of the subsequent mitochondrial alterations that we were going to analyse, we carried out experiments with an exogenous antioxidant (Vit E) which was capable of totally eliminating the excess of free radicals, both ROS (Fig. 1) and $O_2^{\bullet -}$ (Fig. 2c) even with the highest CFU/ml of *H. pylori*.

Cellular antioxidant defense

Mitochondrial electron transport generates superoxide as a by-product and primary ROS at the Complexes I and III. The total $O_2^{\bullet -}$ formation represents more than 1% of O_2 consumption in the electronic transport chain, although the net $O_2^{\bullet -}$ efflux rate are much lower due to its detoxification by matrix and by intramembrane space enzymes. Although GSH/GSSG systems constitute the major redox buffer in the cytosol, mitochondria also appear to have their own GSH pool independent of the cytosolic GSH pool. $O_2^{\bullet -}$ detoxification leading to oxidation of an amount of GSH that is converted in GSSG and GSSG, at the same time, must be reduced to GSH by glutathione reductase with NAD(P)H as a cofactor. If this reduction is not possible, GSH depletion could sensitize cells against apoptotic stimuli [40].

We evaluated GSH and NADPH content in AGS after bacterium infection. NAD(P)H cellular content was calculated according to the difference between the fluorescence intensity values of the samples and of the 70% ethanol-treated cells (mean 49.5 MFI). Controls cells shown a fluorescence mean value of 49.8 MFI, and a mean value of 31.2 MFI was observed in *H. pylori*-infected cells which represented a 37.4% decrease in NAD(P)H content respect to control. With the Vit E pre-treatment the fluorescence mean was 40.3 MFI, a 19.2% decreased compared to control (all $P \leq 0.05$, Fig. 3).

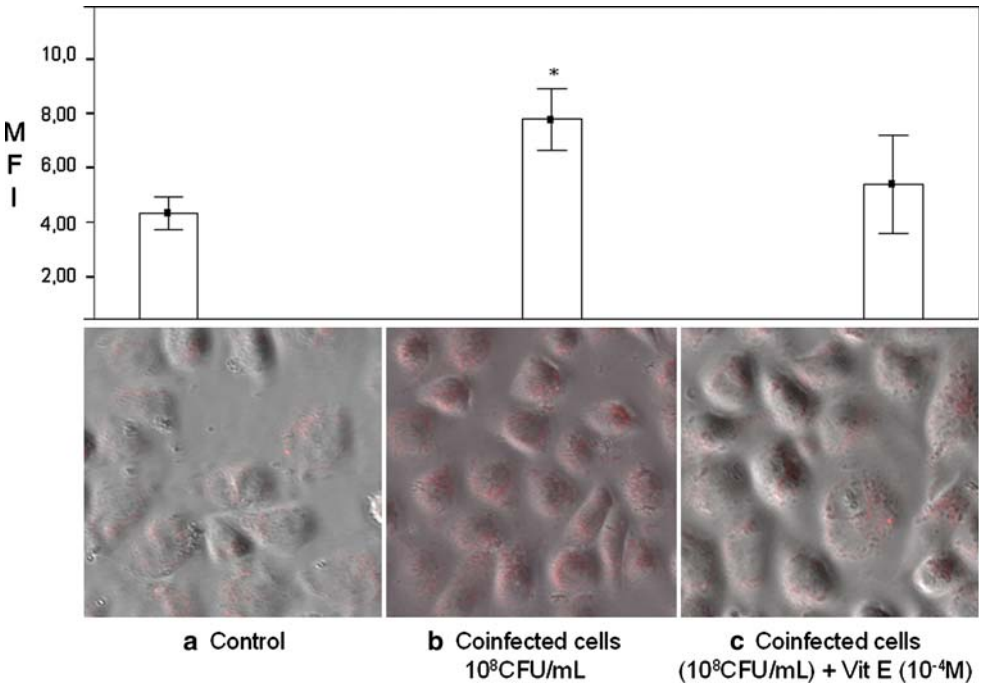

Fig. 2 Superoxide anion production as determined by CM and MitoSOX-staining. Fluorescence was increased in *H. pylori*-infected cells for 24 h (**b**) (7.79 ± 0.89 MFI) compared to controls (**a**) (4.35 ± 0.49 MFI) (*$P \leq 0.05$). The Vit E pre-treatment in cocultures decreased this fluorescence (**c**) (5.41 ± 1.46 MFI). Images were recorded by confocal microscopy (Olympus). Data are ± SD from three independent experiments. Original magnification, ×20 zoom 2

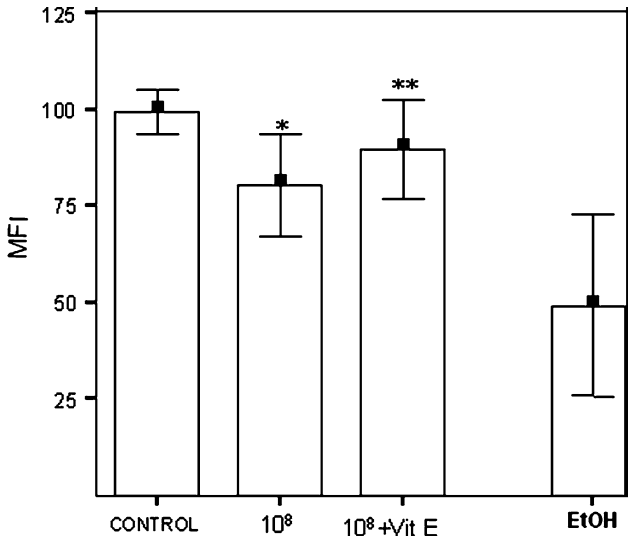

Fig. 3 NAD(P)H cellular content. The coinfected samples for 24 h were exciting with the UV laser in a FACStar Plus. The cell autofluorescence decreased with the coinfection (99.3 ± 3.9 MFI versus 80.7 ± 8.3 MFI) (*$P \leq 0.05$ compared to controls) and part of this autofluorescence was recovered with the Vit E addition (89.8 ± 8.0 MFI) (**$P \leq 0.05$ compared to the coculture). Cells fixed in 70% ethanol were used as a control because they are devoid of NAD(P)H. Data are ± SD from three independent experiments

To evaluate GSH content, we incubated cells with mBBr and found mBBr fluorescence decreased with increased bacterial density (from 1×10^4 to 10^8 CFU/ml). A 31.9% decrease was observed at a MOI of 200:1, whereas the Vit E addition to this concentration counteracted this diminution (all $P \leq 0.05$, Fig. 4).

Cardiolipin peroxidation and mitochondrial structure

Mitochondria are specially sensitive to peroxidation because cardiolipin, the phospholipid most abundant in them, is rich in unsaturated fatty acids.

We evaluated cardiolipin levels as NAO fluorescence (Fig. 5A). After *H. pylori* infection for 24 h the NAO fluorescence of cocultures was found to be significantly lower than control cells (a 40% decrease with 1×10^8 CFU/ml). The Vit E addition counteracted this NAO fluorescence (all $P \leq 0.05$).

Images obtained after NAO staining also allowed us to observe the mitochondrial network disposition (Fig. 5B, top panel). In control cells, the filamentous disposition is located in all the cytoplasma (arrow). In coinfected cells the filaments are broken in round and isolated mitochondria, mainly placed at perinuclear zone, showing a punctuate phenotype (blank arrow). This structural alteration was not observed with *H. pylori* infected cells pretreated with Vit E. *H. pylori* infection also induces cell-size reduction and loss of adhesion as it is observed with phase-contrast microscopy (Fig. 5B, low panel), characteristics associated to hummingbird phenotype described by some authors [41, 42].

Cardiolipin not only interacts with proteins to conserve the structure of multimeric mitochondrial complexes, but also it seems to be involved in early apoptotic events since its oxidation could be essential for the transduction of apoptotic signals such as formation of the mitochondrial permeability transition pore (PTP) that facilitates the release of cyt *c* into the cytosol [43].

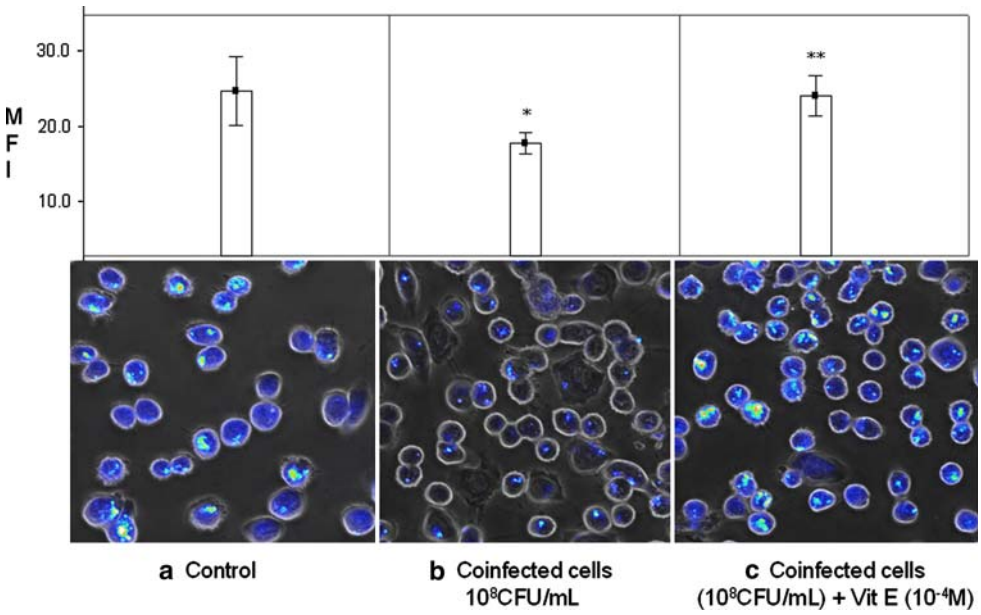

Fig. 4 mBBr staining of thiols detected by CM. A higher content of reduced thiols (e.g., glutathione) was observed in control cells (**a**) versus *H. pylori* treated cells for 24 h (**b**) based on the fluorescence per cell values (16.3 ± 1.5 MFI versus 23.9 ± 5.0 MFI) (*$P \leq 0.05$ compared to controls). Vit E pretreatment prevented the observed decrease in fluorescence (23.3 ± 5.8 MFI) (**$P \leq 0.05$ compared to the coculture) (**c**).Images were recorded by confocal microscopy (Olympus). Each point corresponds to the mean ± SD of three separate experiments. Original magnification, ×20 zoom 2

On the other hand, conditions in which GSH and/or NAD(P)H are depleted, favour mitochondrial-membrane permeabilization via an effect that involves the PTP and the dissipation of $\Delta\psi$m [44].

Mitochondrial membrane potential

We used the fluorescent probe JC-1 to assess whether a $\Delta\psi$m loss was taking place. JC-1, a cationic lipophilic dye becomes concentrated in the mitochondria of healthy cells. This aggregate fluoresces red at higher potential but at lower potential this reagent cannot accumulated in the mitochondria and remains as monomers in the cytoplasm which fluoresces green. The ratio between red and green signals is a measure of $\Delta\psi$m. We observed that the incubation with *H. pylori* modifies the JC-1 green and red fluorescence, creating a 2.8-fold decrease in red/green ratio with 10^8 CFU/ml *H. pylori* (0.43 ± 0.12) compared to control cells (1.20 ± 0.10). This fact suggests that J-aggregates proportion (a structure that is observed in mitochondria, emitting higher levels of red fluorescence emission) is diminished when compared to monomers (structure observed in cytosol exhibiting fluorescence in the green part of the spectrum). And taking into account that fluorocrome accumulation in mitochondria is $\Delta\psi$m dependent, this decrease in the ratio indicates a loss of $\Delta\psi$m. If according to our hypothesis this potential loss is a consequence of oxidative processes derived from the enhanced free radicals synthesis (cardiolipin oxidation and decrease of the reserves of antioxidants), then the Vit E treatment will also be adequate to revert the $\Delta\psi$m decrease. In our experiments the addition of antioxidant nearly restored the ratio (1.09 ± 0.12) to the mean value observed with the control cells (all $P \leq 0.05$, Fig. 6).

Assessment of apoptosis

The previous data indicate that oxidative stress causes alterations in the cell that seem to be related to the programmed cell death. To verify whether apoptotic processes are being produced in cells of our experiments, we analysed the caspase-2 activation, since this molecule participates in proteolytic enzymes cascade initiation in response to pro-apoptotic signals. Moreover, its activation is also related to cytotoxic stress, which is required for the mitochondrial permeabilization, for the release of cyt *c* and for the translocation of Bax from the cytoplasm to mitochondria, features of apoptotic processes by mitochondrial pathway [38]. Data obtained by FC showed that caspase-2 activity, is increased by 33% compared to controls values when bacterial density was 10^8 CFU/ml (201.0 ± 3.6 MFI versus 265.3 ± 22.5 MFI, $P \leq 0.05$). Experiments carried out in Vit E presence corroborated that the caspase-2 activation happened as a result of the increased free radical synthesis, since antioxidant addition to the coculture decreased fluorescence values (237 ± 61.7 MFI). Results were corroborated by CM images, showing a fluorescence increase in infected cells compared to controls ($P \leq 0.05$) and to Vit E-treated cells (Fig. 7).

We additionally assessed the expression levels of executioner caspase-3 (processed downstream of caspase-2 in apoptotic cascade), which is common to both the mitochondria and the death receptor apoptotic pathway. RT-PCR and Western Blot techniques demonstrated an increase in both RNA and protein levels (data not shown).

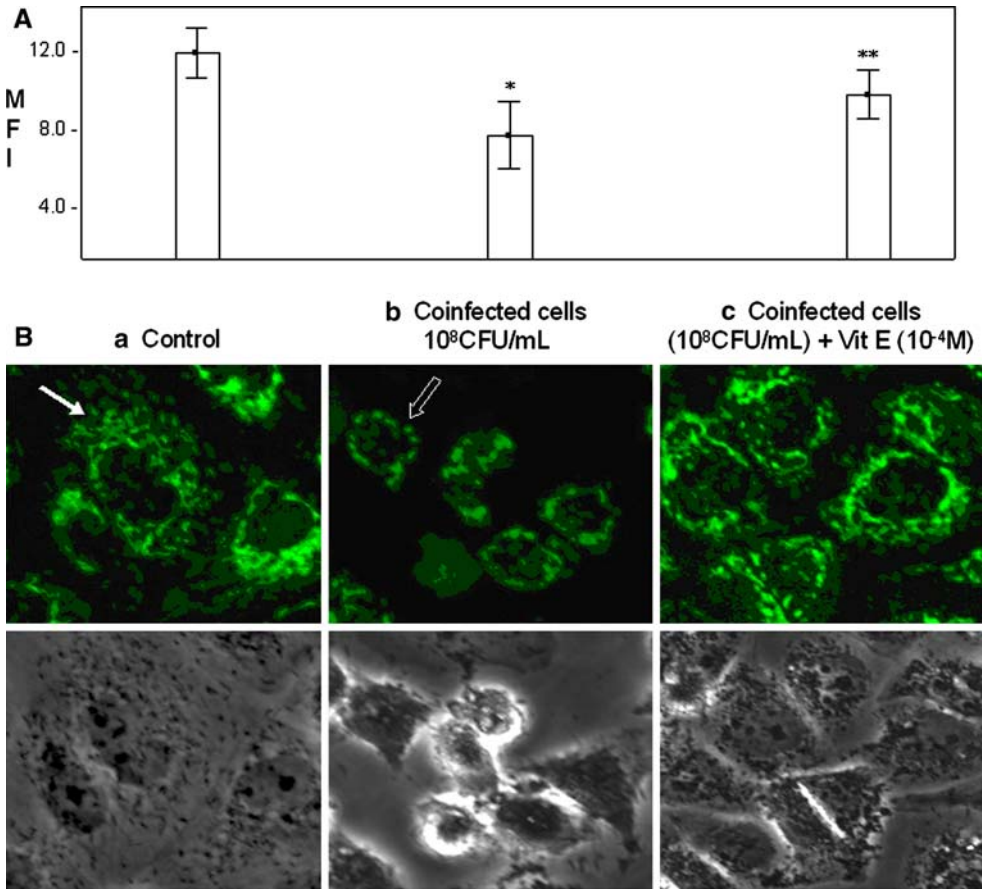

Fig. 5 Cardiolipin content detected by NAO-staining. (**A**) Cardiolipin peroxidation indicated by NAO fluorescence measured at 640 nm is shown. The mean fluorescence values were 6.88 ± 1.16 MFI for cells infected with *H. pylori* for 24 h and 11.41 ± 0.87 MFI for the control cells (*$P \leq 0.05$). Treatment of *H. pylori* infected AGS cells with Vit E increased NAO fluorescence (9.12 ± 0.54 MFI) to a level near that observed with the control cells (**$P \leq 0.05$ compared to the coculture without Vit E). Each point corresponds to the mean ± SD of three independent experiments. (**B**) CM images of NAO-stained cells. Top panel: Appearance of the mitochondrial network. In control cells (a), the mitochondria were arranged as filaments (arrow). After 24 h *H. pylori* infection disrupted this structure by mitochondrial fission generating round and isolated mitochondria (b) (blank arrow). With the Vit E addition the images were similar to controls (c) both in fluorescence and in morphology. Lower panel: The phase-contrast microscopy images display the changes in size and the loss of adhesion of coinfected cells, features that are associated with hummingbird phenotype. Images were recorded by confocal microscopy (Olympus). Representative fields are shown from the results of three separate experiments. Original magnification, ×20 zoom 3

To further confirm that *H. pylori* infection induces apoptotic processes in AGS cells DNA structure was analysed by AO staining and DNA laddering. Nuclear morphology was assessed by adding AO, a nucleic acid selective fluorescent cationic dye, to each well and examining the cells under blue fluorescence. AGS cells used as control displayed normal cellular morphology (homogeneous staining) (Fig. 8a, arrow). In comparison with controls, infected cells displayed features of apoptosis, such as reduced size and enhanced fluorescence of condensed and marginated nuclear chromatin (Fig. 8b, blank arrow), showing a 35% increase of apoptotic cells. Images with the Vit E addition (Fig. 8c) showed the almost total recovery compared to controls (only an 8.3% increase of apoptotic cells) (all $P \leq 0.05$). In coinfected cells, DNA 1.5% agarose gel electrophoresis revealed the formation of DNA fragments of oligonucleosomal size (180–200 bp) (Fig. 9), an observation also consistent with apoptosis.

Discussion

The exact mechanisms by which *H. pylori* colonization causes damage to gastric epithelial cells is unknown, but some hypotheses point at oxidative stress. This oxidative stress is the main consequence of the infiltration of the subepithelial gastric lamina propria by phagocytes, mainly neutrophils and macrophages which produce large amounts of ROS as a host defense reaction.

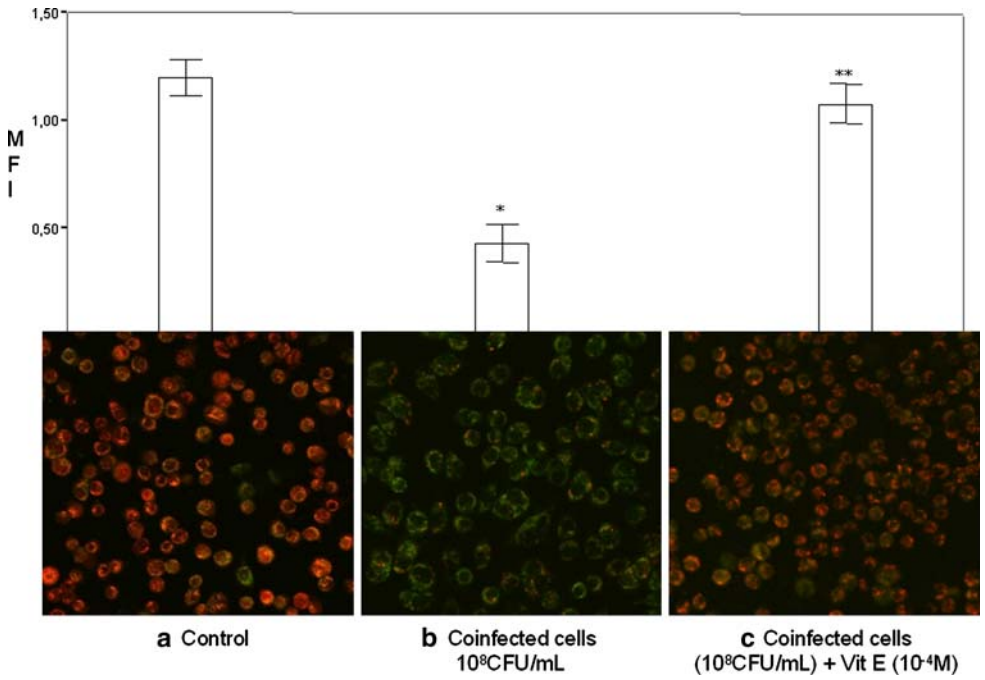

Fig. 6 Mitochondrial membrane potential ($\Delta\psi$m) as determined by CM and JC-1-labelling, calculated as an intensity ratio of JC-1 fluorescence. Control cells (**a**) showed high red and low green fluorescences and cells appeared bright red because of the formation of J-aggregates. In *H. pylori*-treated cells for 24 h (**b**), the JC-1 red/green ratio was reduced by 64.2% (0.43 ± 0.12 MFI) with compared to controls (1.20 ± 0.10 MFI) ($^*P \leq 0.05$) and JC-1 molecules remained as green cytoplasmic monomers. With the antioxidant addition the ratio value was similar to controls (1.09 ± 0.12 MFI) ($^{**}P \leq 0.05$ compared to the coculture) (**c**). Images were recorded by confocal microscopy (Olympus). Data are ± SD from three independent experiments. Original magnification, ×20

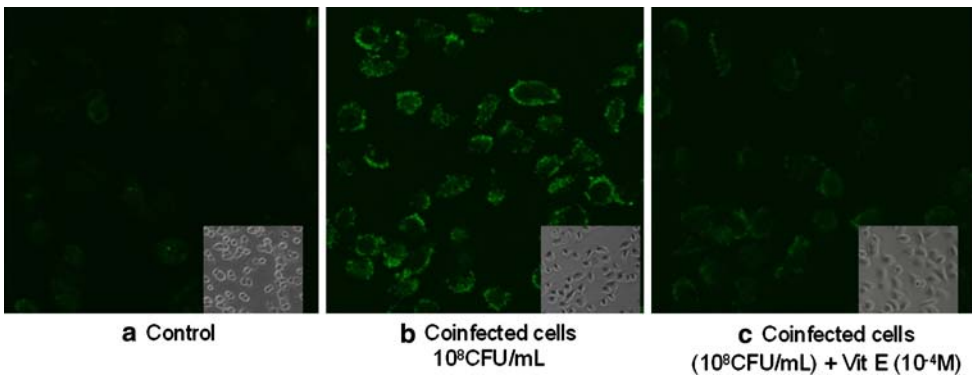

Fig. 7 Caspase-2 detection determined by CM. A 33% increase was observed in caspase-2 activity in cocultures (**b**) for 24 h, measured as FLICA inhibitor fluorescence, compared to controls (**a**) ($P \leq 0.05$). The Vit E addition reverted the fluorescence values to the corresponding controls (**c**) (no statistically significant differences). Images were recorded by confocal microscopy (Olympus). Results are representative of three separate experiments. Original magnification, ×20 zoom 2

In this study we specifically examined mitochondrial alterations at epithelial cell level in response to *H. pylori* infection. Our work is based on the assumption that bacteria produces oxidative stress in the gastric mucosa [7, 45–48] and that mitochondria are one of the possible targets and the major intracellular source of free radicals [49], since it is estimated that 2–4% of the oxygen consumed by mitochondria is converted to $O_2^{\bullet -}$ by the electron transport system [50].

We have been able to show that *H. pylori* causes the buildup of free radicals in epithelial mucosa cells in an infection density-dependent manner, both at the cellular level (Fig. 1) and at the mitochondrial level (Fig. 2). $O_2^{\bullet -}$ is the predominant ROS synthesized in mitochondria [51] and is generated as a by-product of oxidative phosphorylation. Elevated amounts of $O_2^{\bullet -}$ could have detrimental effects on nearby molecules, modifying several proteins of the IMM, lipids or even mitochondrial

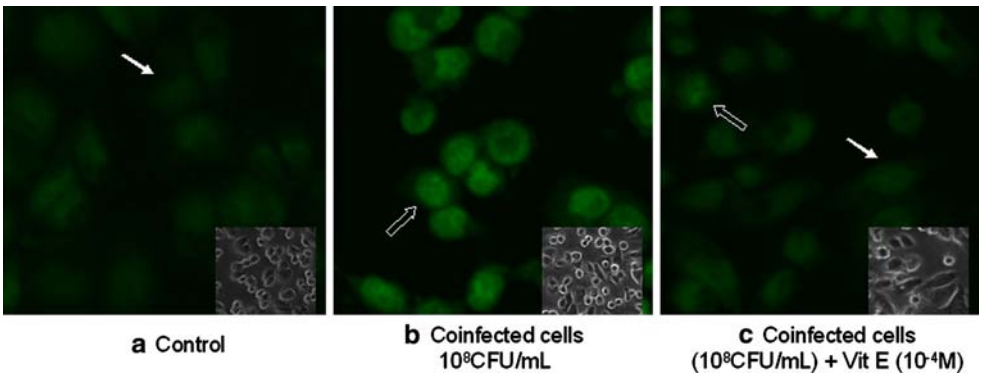

Fig. 8 AO staining of AGS cells evaluated by CM. Nuclei showed green fluorescence. In controls a normal morphology (arrow) with an homogeneous staining is observed (**a**) whereas in the culture with the bacterium for 24 h morphologic features of apoptosis (blank arrow), including condensed and marginated chromatin is observed (**b**). The Vit E partially avoided these alterations (**c**). Data of mean fluorescence per cell were: controls, 2.59 ± 0.16 MFI; coculture, 3.41 ± 0.73 MFI; coculture + Vit E, 2.81 ± 0.70 MFI (all $P \leq 0.05$). Representative fields are shown from the results of three separate experiments. Original magnification, ×20 zoom 2

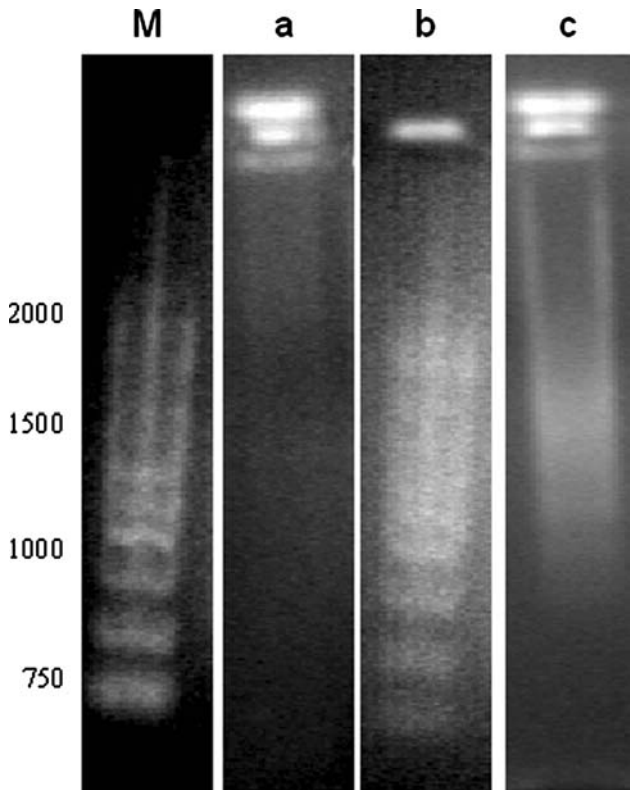

Fig. 9 DNA fragmentation revealed by agarose gel electrophoresis. After 24 h nuclear morphology changes characteristic of apoptosis appear within the cell together with a distinctive biochemical event: the endonuclease-mediated cleavage of nuclear DNA. In apoptotic cells specific DNA cleavage becomes evident in electrophoresis analysis as a typical ladder pattern due to multiple DNA fragments. (M: marker; Lane a: Control; Lane b: coinfected cells; Lane c: coculture + Vit E)

DNA (which has limited protection because of its lack of histones) [52].

In physiological conditions, mitochondria have several enzymes (manganese-dependent superoxide dismutase, glutathione peroxidase) and non-enzimatic systems (NADPH, vitamins C and E) that maintain $O_2^{\bullet -}$ concentrations at very low levels [53, 54]. But when some events cause an overproduction of free radicals, these systems are not able to eliminate the excess. Therefore, overproduction of oxygen radicals may also reduce the antioxidant defenses, and in our experiments, NAD(P)H (Fig. 3) and GSH (Fig. 4) were decreased when cells were *H. pylori*-coinfected.

According to these results, an antioxidant exogenous treatment (Vit E), could prevent damage whether the scavenger was able to eliminate the free radicals excess and recover antioxidant defenses [55, 56]. Our results show that a concentration of 10^{-4} M of Vit E is effective both to remove free radicals synthesized (ROS and $O_2^{\bullet -}$) as a consequence of the infection (Figs. 1 and 2) and to increase antioxidant levels (Figs. 3 and 4). Enzymes such as superoxide dismutase, glutathione peroxidase, catalase, glutathione reductase or transhidrogenase NADP glutathione, and other smaller molecules such as glutathione, NAD(P)H and vitamins C and E are connected and constitute an effective antioxidant system against free radicals. Therefore, when any of these mechanisms are altered, the global systems effectiveness will be modified.

Lipids of cellular membranes are particularly susceptible to oxidation due to the amount of double bonds in these structures. Cardiolipin is an acidic glycerophospholipid that primarily is present in the IMM and is susceptible to lipidic peroxidation, via ROS attack [57], due to two reasons: its unsaturated structure and its location near the place of most cellular $O_2^{\bullet -}$ production, the electron transport system [58]. We show that in *H. pylori*-infected cultures, mitochondria suffer a loss of cardiolipin by peroxidation (Fig. 5A) because when cultures were simultaneously exposed to infection and exogenous treatment with Vit E, a NAO staining pattern was observed that

is similar to control cells. As the ROS burst is concurrent with loss of NAO staining, this event suggests the possibility of a causal relationship.

Cardiolipin is not only an essential phospholipid for eukariotic energy metabolism but also it plays a key role in maintaining mitochondrial structure and function and thus, in cell survival. As CM images shown, our NAO staining experiments revealed that *H. pylori* infection leads to changes in the mitochondrial phenotype (Fig. 5B, top panel): the typical reticulotubular mitochondrial morphology of healthy cells [59] disintegrates into multiple small and round organelles after *H. pylori* infection, rendering the fragmented mitochondrial phenotype that is typical of mitochondrial fission processes. The number and morphology of mitochondria within a cell are controlled by regulated rates of organelle fusion and fission. Any shift in the balance towards fission gives a rise to the fragmentation of the network and remodelling of the mitochondrial cristae observed during the early stages of apoptotic cell death [60–63]. Vit E treatment restored both the mitochondrial (Fig. 5B-c, top panel) and cellular (Fig. 5B-c, low panel) morphology, suggesting that ROS could have an important role in the regulation of fission and fusion processes.

It is also known that mitochondrial uncoupling is associated with increased mitochondrial production of ROS [58]. The passage of electrons along the respiratory chain in mitochondria during oxidative phosphorylation, releases energy and also generates a transmembrane potential gradient across the IMM, but when this process is altered, its potential decreases. AGS infected with *H. pylori* showed a progressive dissipation of $\Delta\psi_m$ (Fig. 6), as determined by the $\Delta\psi_m$-sensitive probe JC-1. It would be reasonable to assume that if these alterations are being triggered by ROS, cellular redox scavengers would tend to prevent them. In our experiments we demonstrate this event because of JC-1 fluorescence red/green ratio in AGS/*H. pylori* cocultures pre-treated with Vit E increased levels as the control cultures (Fig. 6).

All these alterations (oxidative burst, decrease in antioxidant defenses, lipidic oxidation, mitochondrial fission and transmembrane potential dissipation) are related in different clinical conditions with early apoptosis [64]. This is why $\Delta\psi_m$ is lost during the early phase of apoptosis; the outer mitochondrial membrane becomes permeable due to the opening of the mitochondrial PTP that allows the release of soluble intermembrane proteins into the cytosol [65, 66]. The opening of the PTP results in an uncoupling of the respiratory chain and interruption of electron transfer due to the release of intermitochondrial molecules into the cytosol with overproduction of $O_2^{\bullet -}$ [67]. The onset of PTP has been implicated as a key mechanism underlying both necrotic and apoptotic cell death, and ROS are a few of the many agents that promote its opening [68]. PTP activation appears to be irreversible and has profound consequences for cell function [69–71], which is associated with mitochondrial swelling, release of molecules into the cytoplasm, such as apoptosis-inducing factor or cyt *c*, and activation of proteases such as caspases [72, 73], enzymes which participate in a series of reactions that are triggered in response to pro-apoptotic signals. Previous reports have shown that *H. pylori* induces activation of caspase 8 and 3 and subsequent cleavage of PARP, leading to an increased level of apoptosis in gastric ephitelial cells both "in vivo" and "in vitro" [74]. In the present work, we have observed that *H. pylori* plays a role in caspase activation (both at initiator and executioner caspases level), a fact that is, however, antagonized by Vit E (Fig. 7), one of the major lipophilic antioxidant agents, suggesting that ROS are implicated in downstream events leading to an increased level of apoptosis.

It is now clear, that intramitochondrial anti-oxidants such as GSH, NADH, NAD(P)H and superoxide dismutase-Mn are endogenous inhibitors of PTP opening [75, 76] and that conditions in which GSH and/or NAD(P)H are depleted favour mitochondrial-membrane permeabilization via an effect that involves the PTP. NAD(P)H concentrations also appear to be reduced in several models of cell death, and it is accepted that a massive depletion has the same predictive value for cell death as the dissipation of $\Delta\psi_m$ [44].

In addition, the DNA condensation (Fig. 8) and fragmentation (Fig. 9), which are the characteristic morphological features of apoptosis, were detected in AGS infected cells. Features which were inhibited, but not completely abolished, by Vit E. This fact could indicate that other mechanisms, apart from the *H. pylori* induction of ROS synthesis, may be involved in this effect. In fact, some authors have demonstrated that *H. pylori* can directly induce apoptosis of gastric epithelial cells in vitro by Fas/Fas ligand system activation [8, 24, 25, 77]. Our study, however, shows that the mitochondrial pathway plays a critical role in *H. pylori*-mediated apoptosis in gastric epithelial cells.

In summary, our data provide direct information and detailed evidence of how superoxide acts on mitochondria to initiate apoptotic pathways in *H. pylori*-infected AGS cells. These changes are occurring in the presence of mitochondrial depolarisation and other morphological and functional changes. An antioxidant therapy could be useful to the clinical management of infected patients.

Acknowledgements This work was supported in part by a grant 04062-00 from "Instituto de Ciencias de la Salud" J.C.C.M-Spain. M. Calvino was supported by a "Ayuda para incorporación de Jóvenes Investigadores a grupos de investigación de Castilla La Mancha" (JI05000) from J.C.C.M. and by a "Contrato de apoyo a la investigación en el SNS" from Instituto de Salud Carlos III (CA07/00157),

Spain. S. Benito was supported by a "Ayuda para incorporación de Jóvenes Investigadores a grupos de investigación de Castilla La Mancha" (MV2007JI/18) from FISCAM-Spain.

References

1. Allen LA (2000) Modulating phagocyte activation: the pros and cons of *Helicobacter pylori* virulence factors. J Exp Med 191:1451–1454. doi:10.1084/jem.191.9.1451
2. Montecucco C, Rappuoli R (2001) Living dangerously: how *Helicobacter pylori* survives in the human stomach. Nat Rev Mol Cell Biol 2:457–466. doi:10.1038/35073084
3. Willhite DC, Cover TL, Blanke SR (2003) Cellular vacuolation and mitochondrial cytochrome c release are independent outcomes of *Helicobacter pylori* vacuolating cytotoxin activity that are each dependent on membrane channel formation. J Biol Chem 278:48204–48209. doi:10.1074/jbc.M304131200
4. Peek RM Jr, Miller GG, Tham KT et al (1995) Heightened inflammatory response and cytokine expression in vivo to cagA+ *Helicobacter pylori* strains. Lab Invest 73:760–770
5. Blaser MJ, Perez-Perez GI, Kleanthous H et al (1995) Infection with *Helicobacter pylori* strains possessing cagA is associated with an increased risk of developing adenocarcinoma of the stomach. Cancer Res 55:2111–2115
6. Oh TY, Yeo M, Han SU et al (2005) Synergism of *Helicobacter pylori* infection and stress on the augmentation of gastric mucosal damage and its prevention with alpha-tocopherol. Free Radic Biol Med 38:1447–1457. doi:10.1016/j.freeradbiomed.2005.02.005
7. Ding SZ, Minohara Y, Fan XJ et al (2007) *Helicobacter pylori* infection induces oxidative stress and programmed cell death in human gastric epithelial cells. Infect Immun 75:4030–4039. doi:10.1128/IAI.00172-07
8. Jones NL, Day AS, Jennings HA, Sherman PM (1999) *Helicobacter pylori* induces gastric epithelial cell apoptosis in association with increased Fas receptor expression. Infect Immun 67:4237–4242
9. Ashktorab H, Frank S, Khaled AR, Durum SK, Kifle B, Smoot DT (2004) Bax translocation and mitochondrial fragmentation induced by *Helicobacter pylori*. Gut 53:805–813. doi:10.1136/gut.2003.024372
10. Kuck D, Kolmerer B, Iking-Konert C, Krammer PH, Stremmel W, Rudi J (2001) Vacuolating cytotoxin of *Helicobacter pylori* induces apoptosis in the human gastric epithelial cell line AGS. Infect Immun 69:5080–5087. doi:10.1128/IAI.69.8.5080-5087.2001
11. Peek RM Jr, Blaser MJ, Mays DJ et al (1999) *Helicobacter pylori* strain-specific genotypes and modulation of the gastric epithelial cell cycle. Cancer Res 59:6124–6131
12. Fan TJ, Han LH, Cong RS, Liang J (2005) Caspase family proteases and apoptosis. Acta Biochim Biophys Sin (Shanghai) 37:719–727. doi:10.1111/j.1745-7270.2005.00108.x
13. Rudi J, Kuck D, Strand S et al (1998) Involvement of the CD95 (APO-1/Fas) receptor and ligand system in *Helicobacter pylori*-induced gastric epithelial apoptosis. J Clin Invest 102:1506–1514. doi:10.1172/JCI2808
14. Darzynkiewicz Z, Juan G, Li X, Gorczyca W, Murakami T, Traganos F (1997) Cytometry in cell necrobiology: analysis of apoptosis and accidental cell death (necrosis). Cytometry 27:1–20. doi :10.1002/(SICI)1097-0320(19970101)27:1<1::AID-CYTO2>3.0.CO;2-L
15. Palomba L, Sestili P, Columbaro M, Falcieri E, Cantoni O (1999) Apoptosis and necrosis following exposure of U937 cells to increasing concentrations of hydrogen peroxide: the effect of the poly(ADP-ribose)polymerase inhibitor 3-aminobenzamide. Biochem Pharmacol 58:1743–1750. doi:10.1016/S0006-2952(99)00271-3
16. Menaker RJ, Ceponis PJ, Jones NL (2004) *Helicobacter pylori* induces apoptosis of macrophages in association with alterations in the mitochondrial pathway. Infect Immun 72:2889–2898. doi:10.1128/IAI.72.5.2889-2898.2004
17. Maeda S, Yoshida H, Mitsuno Y et al (2002) Analysis of apoptotic and antiapoptotic signalling pathways induced by *Helicobacter pylori*. Mol Pathol 55:286–293. doi:10.1136/mp.55.5.286
18. Maeno E, Ishizaki Y, Kanaseki T, Hazama A, Okada Y (2000) Normotonic cell shrinkage because of disordered volume regulation is an early prerequisite to apoptosis. Proc Natl Acad Sci USA 97:9487–9492. doi:10.1073/pnas.140216197
19. Ormerod MG, Sun XM, Snowden RT, Davies R, Fearnhead H, Cohen GM (1993) Increased membrane permeability of apoptotic thymocytes: a flow cytometric study. Cytometry 14:595–602. doi:10.1002/cyto.990140603
20. Darzynkiewicz Z, Bruno S, Del Bino G et al (1992) Features of apoptotic cells measured by flow cytometry. Cytometry 13:795–808. doi:10.1002/cyto.990130802
21. Koopman G, Reutelingsperger CP, Kuijten GA, Keehnen RM, Pals ST, van Oers MH (1994) Annexin V for flow cytometric detection of phosphatidylserine expression on B cells undergoing apoptosis. Blood 84:1415–1420
22. Zheng TS, Flavell RA (2000) Divinations and surprises: genetic analysis of caspase function in mice. Exp Cell Res 256:67–73. doi:10.1006/excr.2000.4841
23. Walker PR, LeBlanc J, Sikorska M (1997) Evidence that DNA fragmentation in apoptosis is initiated and propagated by single-strand breaks. Cell Death Differ 4:506–515. doi:10.1038/sj.cdd.4400273
24. Houghton J, Korah RM, Condon MR, Kim KH (1999) Apoptosis in *Helicobacter pylori*-associated gastric and duodenal ulcer disease is mediated via the Fas antigen pathway. Dig Dis Sci 44:465–478. doi:10.1023/A:1026628601284
25. Houghton J, Macera-Bloch LS, Harrison L, Kim KH, Korah RM (2000) Tumor necrosis factor alpha and interleukin 1beta up-regulate gastric mucosal Fas antigen expression in *Helicobacter pylori* infection. Infect Immun 68:1189–1195. doi:10.1128/IAI.68.3.1189-1195.2000
26. Zhang H, Fang DC, Lan CH, Luo YH (2007) *Helicobacter pylori* infection induces apoptosis in gastric cancer cells through the mitochondrial pathway. J Gastroenterol Hepatol 22:1051–1056. doi:10.1111/j.1440-1746.2007.04959.x
27. Kim KM, Lee SG, Park MG et al (2007) Gamma-glutamyltranspeptidase of *Helicobacter pylori* induces mitochondria-mediated apoptosis in AGS cells. Biochem Biophys Res Commun 355:562–567. doi:10.1016/j.bbrc.2007.02.021
28. Boya P, Roques B, Kroemer G (2001) New EMBO members' review: viral and bacterial proteins regulating apoptosis at the mitochondrial level. EMBO J 20:4325–4331. doi:10.1093/emboj/20.16.4325
29. Yamasaki E, Wada A, Kumatori A et al (2006) *Helicobacter pylori* vacuolating cytotoxin induces activation of the proapoptotic proteins Bax and Bak, leading to cytochrome c release and cell death, independent of vacuolation. J Biol Chem 281:11250–11259. doi:10.1074/jbc.M509404200
30. Rajalingam K, Oswald M, Gottschalk K, Rudel T (2007) Smac/DIABLO is required for effector caspase activation during apoptosis in human cells. Apoptosis 12:1503–1510. doi:10.1007/s10495-007-0067-7
31. Shirin H, Sordillo EM, Oh SH et al (1999) *Helicobacter pylori* inhibits the G1 to S transition in AGS gastric epithelial cells. Cancer Res 59:2277–2281
32. Bass DA, Parce JW, Dechatelet LR, Szejda P, Seeds MC, Thomas M (1983) Flow cytometric studies of oxidative product

formation by neutrophils: a graded response to membrane stimulation. J Immunol 130:1910–1917
33. Kosower NS, Kosower EM (1987) Thiol labeling with bromobimanes. Methods Enzymol 143:76–84. doi:10.1016/0076-6879(87)43015-2
34. Thorell B (1983) Flow-cytometric monitoring of intracellular flavins simultaneously with NAD(P)H levels. Cytometry 4:61–65. doi:10.1002/cyto.990040109
35. Poot M (2000) Multiparameter analysis of physiological changes in apoptosis. Curr Protoc Cytom 14(Suppl):9.15.11–17
36. Reers M, Smiley ST, Mottola-Hartshorn C, Chen A, Lin M, Chen LB (1995) Mitochondrial membrane potential monitored by JC-1 dye. Methods Enzymol 260:406–417. doi:10.1016/0076-6879(95)60154-6
37. Mileykovskaya E, Dowhan W, Birke RL, Zheng D, Lutterodt L, Haines TH (2001) Cardiolipin binds nonyl acridine orange by aggregating the dye at exposed hydrophobic domains on bilayer surfaces. FEBS Lett 507:187–190. doi:10.1016/S0014-5793(01)02948-9
38. Lassus P, Opitz-Araya X, Lazebnik Y (2002) Requirement for caspase-2 in stress-induced apoptosis before mitochondrial permeabilization. Science 297:1352–1354. doi:10.1126/science.1074721
39. Pomorski T, Meyer TF, Naumann M (2001) *Helicobacter pylori*-induced prostaglandin E(2) synthesis involves activation of cytosolic phospholipase A(2) in epithelial cells. J Biol Chem 276:804–810. doi:10.1074/jbc.M003819200
40. Armstrong JS, Steinauer KK, Hornung B et al (2002) Role of glutathione depletion and reactive oxygen species generation in apoptotic signaling in a human B lymphoma cell line. Cell Death Differ 9:252–263. doi:10.1038/sj/cdd/4400959
41. Segal ED, Cha J, Lo J, Falkow S, Tompkins LS (1999) Altered states: involvement of phosphorylated CagA in the induction of host cellular growth changes by *Helicobacter pylori*. Proc Natl Acad Sci USA 96:14559–14564. doi:10.1073/pnas.96.25.14559
42. Bauer B, Moese S, Bartfeld S, Meyer TF, Selbach M (2005) Analysis of cell type-specific responses mediated by the type IV secretion system of *Helicobacter pylori*. Infect Immun 73:4643–4652. doi:10.1128/IAI.73.8.4643-4652.2005
43. Petrosillo G, Casanova G, Matera M, Ruggiero FM, Paradies G (2006) Interaction of peroxidized cardiolipin with rat-heart mitochondrial membranes: induction of permeability transition and cytochrome c release. FEBS Lett 580:6311–6316. doi:10.1016/j.febslet.2006.10.036
44. Gendron MC, Schrantz N, Metivier D et al (2001) Oxidation of pyridine nucleotides during Fas- and ceramide-induced apoptosis in Jurkat cells: correlation with changes in mitochondria, glutathione depletion, intracellular acidification and caspase 3 activation. Biochem J 353:357–367. doi:10.1042/0264-6021:3530357
45. Obst B, Wagner S, Sewing KF, Beil W (2000) *Helicobacter pylori* causes DNA damage in gastric epithelial cells. Carcinogenesis 21:1111–1115. doi:10.1093/carcin/21.6.1111
46. Smoot DT, Elliott TB, Verspaget HW et al (2000) Influence of *Helicobacter pylori* on reactive oxygen-induced gastric epithelial cell injury. Carcinogenesis 21:2091–2095. doi:10.1093/carcin/21.11.2091
47. Lim JW, Kim H, Kim JM, Kim JS, Jung HC, Kim KH (2004) Cellular stress-related protein expression in *Helicobacter pylori*-infected gastric epithelial AGS cells. Int J Biochem Cell Biol 36:1624–1634. doi:10.1016/j.biocel.2004.01.018
48. Bagchi D, McGinn TR, Ye X et al (2002) *Helicobacter pylori*-induced oxidative stress and DNA damage in a primary culture of human gastric mucosal cells. Dig Dis Sci 47:1405–1412. doi:10.1023/A:1015399204069
49. Teshima S, Rokutan K, Nikawa T, Kishi K (1998) Guinea pig gastric mucosal cells produce abundant superoxide anion through an NADPH oxidase-like system. Gastroenterology 115:1186–1196. doi:10.1016/S0016-5085(98)70090-3
50. Desouki MM, Kulawiec M, Bansal S, Das GM, Singh KK (2005) Cross talk between mitochondria and superoxide generating NADPH oxidase in breast and ovarian tumors. Cancer Biol Ther 4:1367–1373
51. Kudin AP, Bimpong-Buta NY, Vielhaber S, Elger CE, Kunz WS (2004) Characterization of superoxide-producing sites in isolated brain mitochondria. J Biol Chem 279:4127–4135. doi:10.1074/jbc.M310341200
52. Turrens JF (2003) Mitochondrial formation of reactive oxygen species. J Physiol 552:335–344. doi:10.1113/jphysiol.2003.049478
53. Cadenas E, Davies KJ (2000) Mitochondrial free radical generation, oxidative stress, and aging. Free Radic Biol Med 29:222–230. doi:10.1016/S0891-5849(00)00317-8
54. Zhang DX, Gutterman DD (2007) Mitochondrial reactive oxygen species-mediated signaling in endothelial cells. Am J Physiol Heart Circ Physiol 292:H2023–H2031. doi:10.1152/ajpheart.01283.2006
55. Correa P, Malcom G, Schmidt B et al (1998) Review article: antioxidant micronutrients and gastric cancer. Aliment Pharmacol Ther 12(Suppl 1):73–82. doi:10.1111/j.1365-2036.1998.00006.x
56. You WC, Zhang L, Gail MH et al (2000) Gastric dysplasia and gastric cancer: *Helicobacter pylori*, serum vitamin C, and other risk factors. J Natl Cancer Inst 92:1607–1612. doi:10.1093/jnci/92.19.1607
57. Ott M, Gogvadze V, Orrenius S, Zhivotovsky B (2007) Mitochondria, oxidative stress and cell death. Apoptosis 12:913–922. doi:10.1007/s10495-007-0756-2
58. Paradies G, Petrosillo G, Pistolese M, Ruggiero FM (2002) Reactive oxygen species affect mitochondrial electron transport complex I activity through oxidative cardiolipin damage. Gene 286:135–141. doi:10.1016/S0378-1119(01)00814-9
59. Parone PA, Martinou JC (2006) Mitochondrial fission and apoptosis: an ongoing trial. Biochim Biophys Acta 1763:522–530. doi:10.1016/j.bbamcr.2006.04.005
60. Karbowski M, Youle RJ (2003) Dynamics of mitochondrial morphology in healthy cells and during apoptosis. Cell Death Differ 10:870–880. doi:10.1038/sj.cdd.4401260
61. Polyakov VY, Soukhomlinova MY, Fais D (2003) Fusion, fragmentation, and fission of mitochondria. Biochemistry (Mosc) 68:838–849. doi:10.1023/A:1025738712958
62. Lee YJ, Jeong SY, Karbowski M, Smith CL, Youle RJ (2004) Roles of the mammalian mitochondrial fission and fusion mediators Fis1, Drp1, and Opa1 in apoptosis. Mol Biol Cell 15:5001–5011. doi:10.1091/mbc.E04-04-0294
63. Perfettini JL, Roumier T, Kroemer G (2005) Mitochondrial fusion and fission in the control of apoptosis. Trends Cell Biol 15:179–183. doi:10.1016/j.tcb.2005.02.005
64. Rasola A, Bernardi P (2007) The mitochondrial permeability transition pore and its involvement in cell death and in disease pathogenesis. Apoptosis 12:815–833. doi:10.1007/s10495-007-0723-y
65. Isenberg JS, Klaunig JE (2000) Role of the mitochondrial membrane permeability transition (MPT) in rotenone-induced apoptosis in liver cells. Toxicol Sci 53:340–351. doi:10.1093/toxsci/53.2.340
66. Batandier C, Leverve X, Fontaine E (2004) Opening of the mitochondrial permeability transition pore induces reactive oxygen species production at the level of the respiratory chain complex I. J Biol Chem 279:17197–17204. doi:10.1074/jbc.M310329200

67. Cai J, Jones DP (1998) Superoxide in apoptosis. Mitochondrial generation triggered by cytochrome c loss. J Biol Chem 273:11401–11404. doi:10.1074/jbc.273.19.11401
68. Kim JS, He L, Lemasters JJ (2003) Mitochondrial permeability transition: a common pathway to necrosis and apoptosis. Biochem Biophys Res Commun 304:463–470. doi:10.1016/S0006-291X(03)00618-1
69. Justo P, Lorz C, Sanz A, Egido J, Ortiz A (2003) Intracellular mechanisms of cyclosporin A-induced tubular cell apoptosis. J Am Soc Nephrol 14:3072–3080. doi:10.1097/01.ASN.0000099383.57934.0E
70. Brenner C, Grimm S (2006) The permeability transition pore complex in cancer cell death. Oncogene 25:4744–4756. doi:10.1038/sj.onc.1209609
71. Grimm S, Brdiczka D (2007) The permeability transition pore in cell death. Apoptosis 12:841–855. doi:10.1007/s10495-007-0747-3
72. Kroemer G, Reed JC (2000) Mitochondrial control of cell death. Nat Med 6:513–519. doi:10.1038/74994
73. Xia T, Jiang C, Li L, Wu C, Chen Q, Liu SS (2002) A study on permeability transition pore opening and cytochrome c release from mitochondria, induced by caspase-3 in vitro. FEBS Lett 510:62–66. doi:10.1016/S0014-5793(01)03228-8
74. Ashktorab H, Neapolitano M, Bomma C et al (2002) In vivo and in vitro activation of caspase-8 and -3 associated with *Helicobacter pylori* infection. Microbes Infect 4:713–722. doi:10.1016/S1286-4579(02)01591-5
75. Zago EB, Castilho RF, Vercesi AE (2000) The redox state of endogenous pyridine nucleotides can determine both the degree of mitochondrial oxidative stress and the solute selectivity of the permeability transition pore. FEBS Lett 478:29–33. doi:10.1016/S0014-5793(00)01815-9
76. Aronis A, Komarnitsky R, Shilo S, Tirosh O (2002) Membrane depolarization of isolated rat liver mitochondria attenuates permeability transition pore opening and oxidant production. Antioxid Redox Signal 4:647–654. doi:10.1089/15230860260220157
77. Takeda K, Akira S (2003) Toll receptors and pathogen resistance. Cell Microbiol 5:143–153. doi:10.1046/j.1462-5822.2003.00264.x